The Astrophysical Journal, 757:180 (10pp), 2012 October 1 doi:10.1088/0004-637X/757/2/180
© 2012. The American Astronomical Society. All rights reserved. Printed in the U.S.A.

THE INTRINSIC FRACTIONS AND RADIO PROPERTIES OF LOW-IONIZATION BROAD ABSORPTION LINE QUASARS

Xinyu Dai[1], Francesco Shankar[2], and Gregory R. Sivakoff[3]
[1] Homer L. Dodge Department of Physics and Astronomy, University of Oklahoma, Norman, OK 73019, USA; xdai@ou.edu
[2] GEPI, Observatoire de Paris, CNRS, University of Paris Diderot, 5 Place Jules Janssen, F-92195 Meudon, France
[3] Department of Physics, University of Alberta, Edmonton, AB T6G 2E1, Canada
Received 2012 April 5; accepted 2012 August 24; published 2012 September 17

ABSTRACT

Low-ionization (Mg II, Fe II, and Fe III) broad absorption line quasars (LoBALs) probe a relatively obscured quasar population and could be at an early evolutionary stage for quasars. We study the intrinsic fractions of LoBALs using the Sloan Digital Sky Survey (SDSS), Two Micron All Sky Survey, and Faint Images of the Radio Sky at Twenty cm survey. We find that the LoBAL fractions of the near-infrared (NIR) and radio samples are approximately 5–7 times higher than those measured in the optical sample. This suggests that the fractions measured in the NIR and radio bands are closer to the intrinsic fractions of the populations, and that the optical fractions are significantly biased due to obscuration effects, similar to high-ionization broad absorption line quasars (HiBALs). Considering a population of obscured quasars that do not enter the SDSS, which could have a much higher LoBAL fraction, we expect that the intrinsic fraction of LoBALs could be even higher. We also find that the LoBAL fractions decrease with increasing radio luminosities, again, similarly to HiBALs. In addition, we find evidence for increasing fractions of LoBALs toward higher NIR luminosities, especially for FeLoBALs with a fraction of $\sim$18% at $M_{K_s} < -31$ mag. This population of NIR-luminous LoBALs may be at an early evolutionary stage of quasar evolution. To interpret the data, we use a luminosity-dependent model for LoBALs that yields significantly better fits than those from a pure geometric model.

Key words: galaxies: active – galaxies: evolution – quasars: absorption lines – quasars: general

Online-only material: color figures

1. INTRODUCTION

Broad absorption line quasars (BALQSOs) are a sub-sample of quasars exhibiting blueshifted absorption troughs (e.g., Weymann et al. 1991). In the traditional definition of Weymann et al. (1991), absorption troughs must be at least 2000 km s^{-1} wide excluding the first 3000 km s^{-1} region blueward from the emission lines to classify quasars as BALQSOs. Less strict definitions have also been used, for example, with a requirement of a trough to be at least 1000 km s^{-1} wide (e.g., Trump et al. 2006). BALQSOs can also be further divided into a population containing absorption troughs from only high-ionization state species (e.g., C IV and N V; high-ionization broad absorption line quasars, HiBALs) and a population that exhibits absorption troughs in low-ionization species (e.g., Mg II and Fe II; low-ionization broad absorption line quasars, LoBALs). The majority of BALQSOs are HiBALs. In fact, all LoBALs also contain the high-ionization troughs in their spectra (e.g., Weymann et al. 1991; Trump et al. 2006). Besides the presence of low-ionization troughs, the optical continua of LoBALs are more reddened compared to HiBALs, suggesting stronger dust extinction (e.g., Sprayberry & Foltz 1992; Reichard et al. 2003). In X-rays, LoBALs also have higher gas absorption column densities than HiBALs (e.g., Green et al. 2001; Gallagher et al. 2002). Therefore, LoBALs probe a relatively obscured quasar population. The origin of a small LoBAL fraction in quasars is unclear, and it has been attributed to geometric effects (e.g., Elvis 2000) or evolutionary effects (e.g., Voit et al. 1993), like the BALQSO population in general. There are several tentative arguments supporting the view that LoBALs are young quasars at a stage of blowing out obscuring materials. First, several early studies of LoBAL fractions in the infrared band showed larger fractions (e.g., Boroson & Meyers 1992) and associations with ultraluminous infrared galaxies (e.g., Lipari 1994; Canalizo & Stockton 2000). Second, a few optical spectral analyses suggested that the covering fraction of the LoBAL wind is large (e.g., Voit et al. 1993; Casebeer et al. 2008). Third, some radio spectra of LoBALs resemble those of compact steep-spectrum or gigahertz-peaked spectrum sources, which are also candidates for young quasars (e.g., Montenegro-Montes et al. 2008; Liu et al. 2008). In particular, the LoBALs containing Fe absorption troughs (FeLoBAL) are viewed as the most promising candidates for young quasars (e.g., Lipari et al. 2009). The fractions of LoBALs are important constraints on the origin of the LoBAL populations.

Before studying the intrinsic fractions of LoBALs, it is important to compare the measurements of the intrinsic fractions of BALQSOs in the quasar population. Recently, a series of studies emerged on this topic. Dai et al. (2008b) studied the Sloan Digital Sky Survey (SDSS) BALQSO (Trump et al. 2006) fractions in the Two Micron All Sky Survey (2MASS) bands (Skrutskie et al. 2006), finding that the BALQSO fractions in the near-infrared (NIR) are twice those found in the optical band. In particular, we found the BALQSO fraction to be 20% $\pm$ 2% for the traditional BALQSOs that satisfy the stricter Weymann et al. (1991) definition and 43% $\pm$ 2% for the relaxed definition of Trump et al. (2006) that requires less broad absorption troughs. Dai et al. (2008b) argued that the BALQSO fractions measured in the NIR bands are closer to the intrinsic fractions, based on the observation that significant obscuration is associated with BALQSOs in the optical bands (e.g., Reichard et al. 2003), confirming the earlier estimate of Hewett & Foltz (2003). This result was confirmed by several studies, such as Ganguly & Brotherton (2008) using a different SDSS BALQSO catalog,

Maddox et al. (2008) using the deeper UKIDSS survey, Shankar et al. (2008b) in the radio band, and Knigge et al. (2008) by correcting the fraction in the optical bands directly. In particular, Ganguly & Brotherton (2008) extended the study to include narrow and associated absorbers and found the overall outflowing active galactic nuclei (AGNs) to be 60% of the total quasar population. Recently, Allen et al. (2011) claimed an even larger intrinsic fraction for the traditional BALQSOs of 41%, by including the additional fraction of missing quasars that do not enter the SDSS. In particular, Allen et al. (2011) found that the completeness for BALQSOs and non-BALQSOs in SDSS is very similar at $z < 2.1$ and $z > 3.6$ but can differ at other redshifts, e.g., for $z \sim 2.6$ and $z \sim 3.5$ (at least for quasars whose other properties, in particular the level of dust extinction, are the same).

The larger fraction of BALQSOs makes the AGN wind a more promising candidate responsible for the feedback energy that is needed to explain the co-evolution between black holes and their host galaxies. Understanding evolutionary versus geometric models of AGNs can not only probe the AGN feedback but also constrain the nature of the feedback, whether it is kinetic from winds (e.g., Granato et al. 2004; Shankar et al. 2006, 2008a) or thermal (e.g., Di Matteo et al. 2005; Hopkins et al. 2006). If BALQSOs provide the majority of the feedback energy, the feedback mechanism will be kinetic. Motivated by the results from BALQSOs and the larger obscuration of LoBALs compared to HiBALs, we expect that the optical fractions for LoBALs are also biased low. This effect has already been noticed when only a few LoBALs were observed (Sprayberry & Foltz 1992); however, their study was limited by their small sample size. The large sample size enabled by SDSS warrants a new study on the intrinsic fractions of LoBALs.

The radio properties of BALQSOs provide additional constraints on the nature of these objects. In an early study, Stocke et al. (1992) found no radio-loud BALQSOs within 68 BALQSOs. Later studies showed that radio emission is present in BALQSOs (Francis et al. 1993; Brotherton et al. 1998; Becker et al. 2000); however, these BALQSOs are mostly radio-moderate. Matching the SDSS BALQSO catalog in the Faint Images of the Radio Sky at Twenty cm (FIRST) survey (Becker et al. 1995), Shankar et al. (2008b) quantified the dependence of the BALQSO fraction on radio luminosities. We found that the BALQSO fraction drops at high radio luminosities, confirming earlier claims of such an effect (Stocke et al. 1992; Becker et al. 2000, 2001). In addition, Shankar et al. (2008b) also found that the BALQSO fraction at the low radio luminosity range is consistent with the NIR fraction of BALQSOs of Dai et al. (2008b). This result further supports the view that the NIR BALQSO fraction is close to the intrinsic fraction (modulo corrections to the parent SDSS quasar selection), since there is also little absorption in the radio bands. The drop of the BALQSO fractions at high radio luminosities can be naturally explained under a geometric model of BALQSOs. If the radio emission has a preferred orientation, which is usually considered in the polar direction, the drop indicates that BALQSOs are less frequent in these viewing angles. Using a unification model between radio-loud and radio-quiet quasars (e.g., Urry & Padovani 1995), we were able to successfully reproduce the trend, thus explaining the majority of the BALQSOs with radio emission under a geometric model. Exceptions still exist, such as the polar radio-loud BALQSOs, which were identified based on the radio variability that implies too large brightness temperatures unless the radio emission is relativistic (e.g., Zhou et al. 2006; Ghosh & Punsly 2007). Cold polar outflows are also present in blazars (e.g., Dai et al. 2008a), and they could be related to polar BALQSOs as the outflow continuously extends close to the polar axis. However, these objects are rare, and their implication for the total BALQSO population is still uncertain.

In this paper, we study the intrinsic fraction of LoBALs by correlating SDSS quasars with detections in the NIR and radio bands. We also explore their radio properties and compare with BALQSOs to test whether LoBALs can be explained under a geometric or evolutionary model. We assume that $H_0 = 70\,\mathrm{km\,s^{-1}\,Mpc^{-1}}$, $\Omega_\mathrm{m} = 0.3$, and $\Omega_\Lambda = 0.7$ throughout the paper.

2. SAMPLE SELECTION

We select quasars from the SDSS DR3 quasar catalog (Schneider et al. 2005) and the SDSS-BALQSO catalog (Trump et al. 2006, T06 hereafter), where the authors also separately tagged the LoBAL population. In particular, we study quasars in the redshift range of $0.5 \leqslant z \leqslant 2.15$, where the Mg II absorption line falls in the observed-frame optical band pass. Note that, in this redshift range, the completeness of BALQSOs and non-BALQSOs is very similar for the SDSS (Allen et al. 2011). For the FeLoBAL sample, we study the quasars in the redshift range of $1.19 \leqslant z \leqslant 2.24$, which is the redshift range of FeLoBALs identified in T06. Following Dai et al. (2008b) and Shankar et al. (2008b), we match the quasars using a $2''$ radius to entries from the full 2MASS release, which extends to fluxes below the official completeness level of the 2MASS All-Sky Point Source Catalog. To ensure that the matched database entries represent detections, we require an in-band detection (rd_flg != 0) that there is no confusion, contamination (cc_flg == 0), or blending (bl_flg $\leqslant$ 1) in the source, and that no source is near an extended galaxy (gal_contam == 0 and ext_key is null). The 99% completeness levels of the database are $J = 16.1$, $H = 15.5$, and $K_s = 15.1$ mag. Recently, several new BALQSO catalogs have been published using more recent SDSS data releases (Gibson et al. 2009, G09 hereafter; Scaringi et al. 2009; Allen et al. 2011). In particular, the catalog of G09 also provides identifications of traditional Mg II LoBALs in the redshift range of $0.55 \leqslant z \leqslant 2.15$. We also briefly present the analysis to this sample as a comparison. We mainly present results based on the T06 sample, unless mentioned otherwise.

Following Shankar et al. (2008b, 2010), we build a full FIRST–SDSS cross-correlation catalog, containing all the detected radio components within $30''$ of an optical quasar. As our reference, following Schneider et al. (2005), we primarily present results for the FIRST–SDSS catalog with radio counterparts identified within $2''$. We also test our results by enlarging the radio matches to $5''$, and the results are consistent with those from the $2''$ matching. In addition, many of the optical sources in SDSS are associated with more than one radio component in FIRST within $30''$, as expected if these sources are extended with jets and/or lobes separated from the central source. We use the sum of the flux densities as a proxy for the total radio luminosity of these sources. We require that at least one component is within our matching radius for the cases of multiple source matches. Although SDSS targets radio sources serendipitously, we find no unusual agglomerations or bimodalities in the radio flux of SDSS quasars, especially at low flux levels.

In the rest of the paper, we refer to LoBALs that satisfy the traditional definition of Weymann et al. (1991) as "BI-LoBALs," to LoBALs that are selected from T06 using

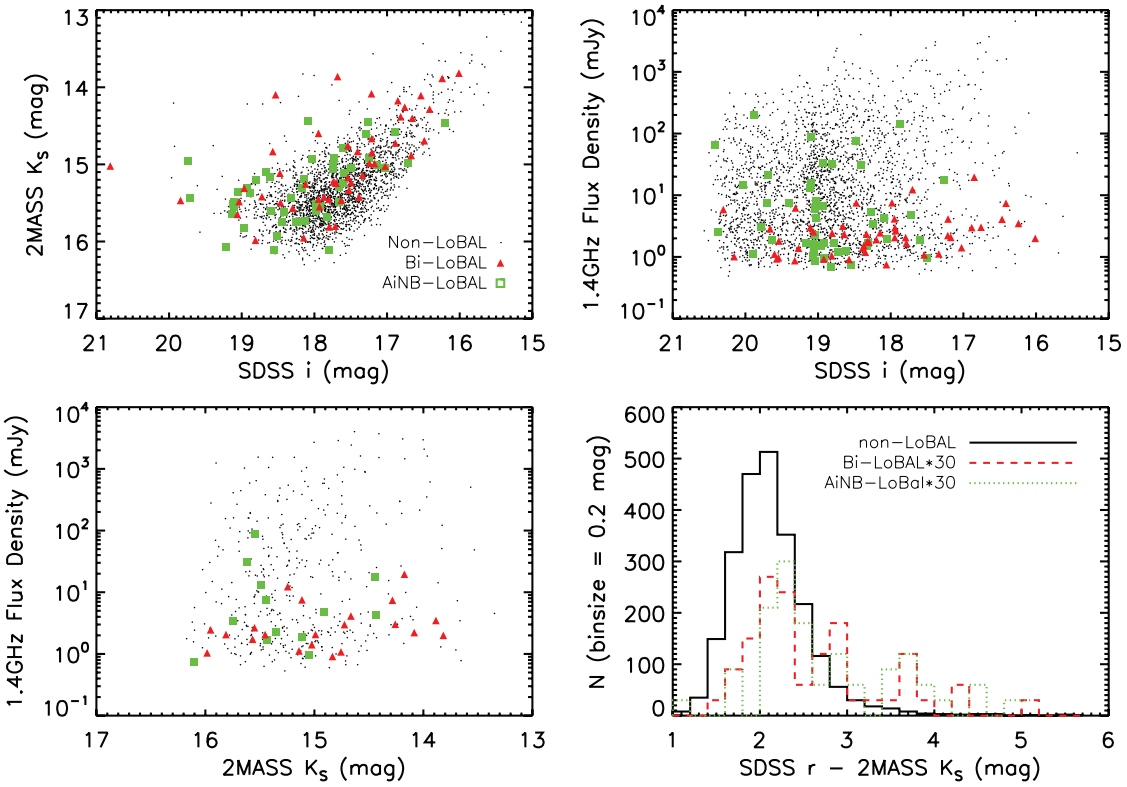

Figure 1. Top left: 2MASS K_s magnitude vs. SDSS i magnitude for SDSS DR3 QSOs that are detected in all of the J, H, and K_s bands in the redshift range of $0.5 \leqslant z \leqslant 2.15$. The sub-samples of QSOs that are not LoBALs (non-LoBALs; black dots), QSOs that satisfied the traditional Weymann et al. definition (BI-LoBALs; red triangles), and QSOs that satisfied the relaxed BAL definition of Trump et al. (2006) but did not satisfy the traditional definition (AINB-LoBALs; green squares) are displayed separately. Top right: SDSS i magnitude vs. 1.4 GHz flux density. Bottom left: 2MASS K_s magnitude vs. 1.4 GHz flux density. Bottom right: SDSS $r-$2MASS K_s color for the three samples, where the histograms for the two LoBAL samples are multiplied arbitrarily by 30 for clarity. The LoBALs are significantly redder than the non-LoBAL population.

(A color version of this figure is available in the online journal.)

the relaxed AI definition as "AI-LoBALs," to LoBALs that satisfy the relaxed AI definition but not the traditional definition as "AINB-LoBALs," and to the rest of the sample without LoBAL features as "non-LoBALs." Some studies have found that the AINB sample has properties besides the absorption troughs that differ from the BI sample, which may indicate a separate population (e.g., Knigge et al. 2008; Shankar et al. 2008b). We note that at the redshift ranges we study, the SDSS spectra cannot separate all the HiBALs from non-BALs because the high-ionization troughs are not redshifted into the optical spectral range. We also refer to the "2MASS sample" as quasars detected in all of the J, H, and K_s bands, and to the "K_s complete sample" as quasars with $K_s < 15.1$ mag. We test our results using the two samples, and they are not qualitatively different. Because of the scarcity of LoBALs, we choose to mainly present the results from the 2MASS sample to reduce the uncertainties of our fraction measurements.

3. RESULTS

3.1. Distributions of LoBALs in the Optical, NIR, and Radio Bands

We compare the optical, near-IR, and radio properties of various LoBALs in Figures 1 and 2. In three panels of Figure 1, we plot the SDSS i magnitude, 2MASS K_s magnitude, and FIRST 1.4 GHz flux density against each other for three samples, BI-LoBALs, AINB-LoBALs, and non-LoBALs. The distributions of LoBAL samples are different from the non-LoBAL sample in all three cases. In the K_s- versus i-magnitude plot (Figure 1, top left), the quasars are concentrated in a linear relation between the i and K_s magnitudes with scatter. We can see that the LoBALs in the plot are systematically redder than the non-LoBAL population, as expected since the optical spectra of LoBALs show extra dust extinction compared to HiBALs and non-BALs (e.g., Reichard et al. 2003). We note that some of the scatter is due to quasar variability, since the SDSS and 2MASS data are taken from different epochs. However, this should not affect the mean color difference between the LoBALs and non-LoBALs in the plot. In the two panels involving radio flux in Figure 1, we clearly see that the LoBALs are less populated in the high radio flux regime. In the bottom-right panel of Figure 1, we show the histograms of the SDSS $r-$2MASS K_s color for the BI-LoBALs, AINB-LoBALs, and non-LoBALs in our sample as another example to demonstrate the redder color of the LoBAL population. Since the $r - K_s$ color also depends on the quasar redshift, a small part of the spread in the $r - K_s$ color distribution is caused by the redshift distribution of our sample. We have removed this redshift dependence in Figure 1 (bottom right) by calculating the $r - K_s$ colors relative to the mean $r - K_s$ color from a sub-sample of non-LoBALs with redshift close to the mean of our redshift distribution. We also show the cumulative distribution of the $r - K_s$ color in Figure 3 and perform the Kolmogorov–Smirnov (K-S) test on the distributions. The K-S test results show that the AI-LoBALs of our sample are significantly different from the non-LoBALs with a very small probability (3×10^{-13}) for the two populations to arise from the same parent distribution. The situation is the same when we compare the sub-populations of the AI-LoBALs

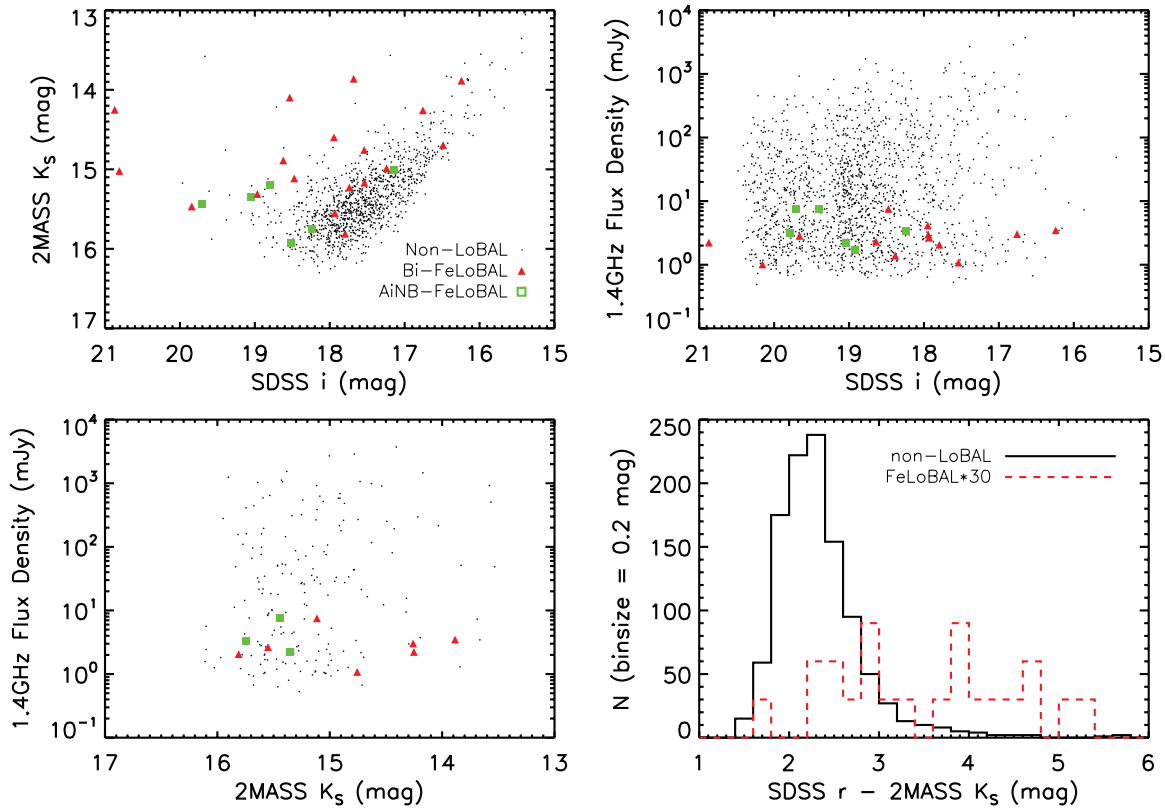

Figure 2. Same plots as Figure 1, but for FeLoBALs in the redshift range of $1.19 \leqslant z \leqslant 2.24$. The FeLoBALs are also significantly redder than the non-LoBAL population.

(A color version of this figure is available in the online journal.)

(BI-LoBALs and AINB-LoBALs) with the non-LoBALs, where we obtain K-S probabilities of 2×10^{-5} and 2×10^{-9}. Comparing the BI-LoBALs and AINB-LoBALs in the plot, we find that the two color distributions are not significantly different, with a K-S probability of 0.38. In Figure 2, we compare the properties of the FeLoBALs and non-LoBALs of our sample using the same axes as in Figure 1. We find that FeLoBALs are also more reddened than non-LoBALs, BALs, and LoBALs, as expected. The radio powers of the FeLoBALs in the plot are similar to those of the BI-LoBALs.

3.2. The Intrinsic Fraction of LoBALs

We present the fraction of LoBALs (BI-LoBALs, AI-LoBALs, and FeLoBALs) measured in the SDSS and 2MASS g, r, i, z, J, H, and K_s bands in Figures 4 and 6 (left). We also list the numbers and fractions of LoBALs in Table 1, where we use Gehrels's statistics to estimate the uncertainties (Gehrels 1986). We first calculate the absolute magnitudes of the quasars in the SDSS and 2MASS bands correcting for the k-correction and the Galactic extinction, but not correcting for the obscuration in the BALQSOs. Although the Hα line can contribute to a fraction of the flux in one of the 2MASS bands, because the 2MASS bands are quite broad, this will only modestly affect our results. We then calculate the fraction in the K_s band with an absolute magnitude limit of $M_{K_s} \leqslant -29.5$ mag. For the rest of the bands, we set the limits so that the differences between the band limits are the same as their mean color differences, i.e., $M_{X,\rm lim} - M_{Y,\rm lim} = \overline{M_X - M_Y}$. We find that the LoBAL fractions are increasing from blue to red bands, similar to the results for BALQSOs (Dai et al. 2008b). This trend can be naturally explained considering the significant obscuration in LoBALs compared to HiBALs and non-BALs (e.g., Sprayberry & Foltz 1992), and the implication is that the 2MASS fractions are closer to the intrinsic fraction of these objects. Comparing the BI-LoBAL samples from T06 and G09, we find that the overall trend is consistent between the two samples. However, there is a systematic offset between the two samples, where the T06 sample has higher fractions due to the relatively less restrictive LoBAL identification criterion.

Following Dai et al. (2008b), we test the obscuration model by combining the quasar luminosity function (Richards et al. 2005) and the spectral differences between LoBALs, HiBALs, and non-BALs (Reichard et al. 2003), Model I hereafter. We assume that LoBALs, HiBALs, and non-BALs have the same intrinsic luminosity functions $\Phi(L) \propto L^{-\alpha}$, where we set $\alpha = 3.31$, (e.g., Richards et al. 2005), with the only difference being in their normalizations. Since LoBALs and HiBALs are obscured, their observed luminosity functions are horizontally shifted to be less luminous, where the shift corresponds to the mean obscuration caused by dust extinction and absorption. The shift caused by obscuration is smaller in the red bands and larger in the blue bands. We calculate the obscuration based on the SDSS composite spectral models (Reichard et al. 2003). Since our sample spans a large redshift range, we find the average obscuration in the range for the simulations. In addition, our results will also be affected if the distribution of the obscuration is quite skewed. However, since we do not know this distribution, we model the obscuration using a simple mean. Finally, we calculate the model observed fraction of LoBALs in the SDSS and 2MASS bands and compare with the observations. The only free parameter is the intrinsic fraction of LoBALs. Please refer

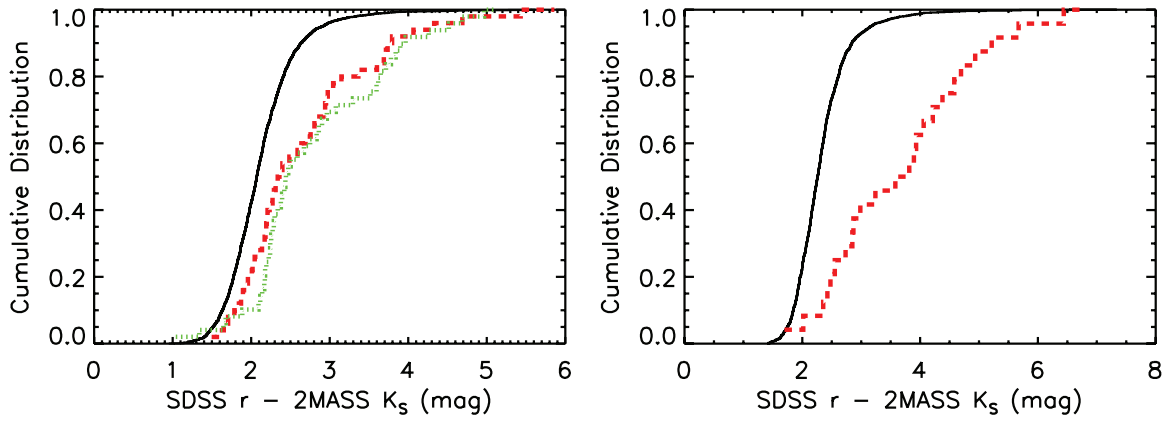

Figure 3. Cumulative distributions of the SDSS $r - 2$MASS K_s color for the LoBAL samples. The left panel shows the distributions for non-LoBALs (solid), BI-LoBALs (dashed), and AINB-LoBALs (dotted), respectively. The K-S test results indicate that both of the LoBAL samples differ from the non-LoBAL sample with significances greater than 99.998%, and that the two LoBAL samples are not significantly different from each other. The right panel shows distributions for non-LoBALs (solid) and FeLoBALs (dashed). The K-S test result indicates that the $r - K_s$ colors of the FeLoBAL population differ from those of the non-LoBAL population with a significance greater than (1–2) $\times 10^{-10}$.

(A color version of this figure is available in the online journal.)

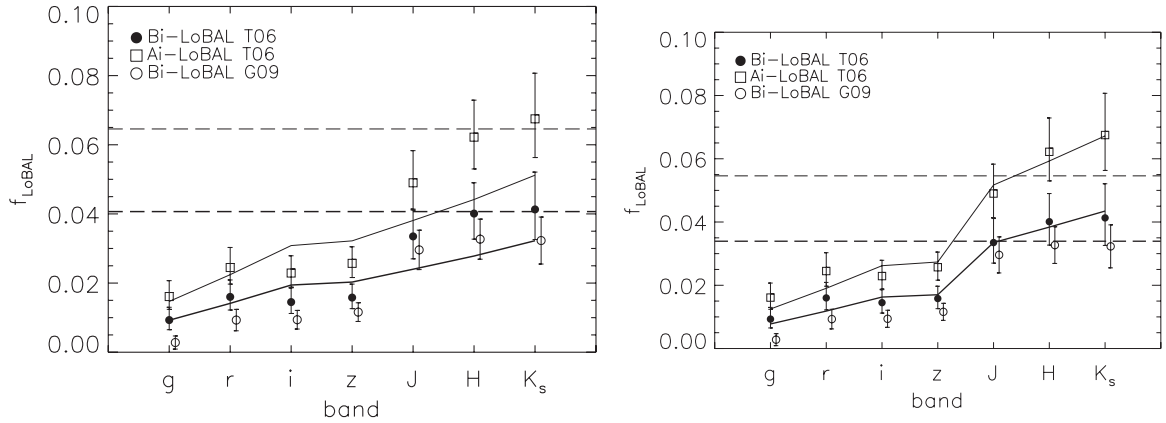

Figure 4. Left: observed LoBAL fractions in optical and infrared bands. The filled circles and open squares are the observed BI-LoBAL and AI-LoBAL fractions from T06, and the open circles are from G09, where we shift the G09 data slightly to the right for clarity. The BAL fractions increase from the blue to red bands, and the fractions can be modeled assuming that there is significant obscuration in LoBALs. The heavy dashed line is the model intrinsic fraction for BI-LoBALs of T06, and the light dashed line is for that of AI-LoBALs of T06. The solid lines are the modeling results for the observed fractions. Right: we add an additional component of LoBALs at high luminosities to our model, where we obtain better fits to the data. The dashed lines show the ratios of the normalizations in the LoBAL and the total quasar luminosity functions.

Table 1
Fractions of LoBALs in the 2MASS and SDSS Bands

	Sample	Redshift Range	u	g	r	i	z	J	H	K_s
Limiting mag			−26.7	−26.9	−27.1	−27.2	−27.2	−28.3	−28.9	−29.5
N (Total)	T06	0.50–2.15	1460	1181	1062	1312	1518	776	724	533
N (BI-LoBAL)			5	11	17	19	24	26	29	22
f (BI-LoBAL)			$0.3^{+0.2}_{-0.2}$	$0.9^{+0.4}_{-0.3}$	$1.6^{+0.5}_{-0.4}$	$1.5^{+0.4}_{-0.3}$	$1.6^{+0.4}_{-0.3}$	$3.4^{+0.8}_{-0.7}$	$4.0^{+0.9}_{-0.7}$	$4.1^{+1.1}_{-0.9}$
N (AI-LoBAL)			12	19	26	30	39	38	45	36
f (AI-LoBAL)			$0.8^{+0.3}_{-0.2}$	$1.6^{+0.5}_{-0.4}$	$2.5^{+0.6}_{-0.5}$	$2.3^{+0.5}_{-0.4}$	$2.6^{+0.5}_{-0.4}$	$4.9^{+0.9}_{-0.8}$	$6.2^{+1.1}_{-0.9}$	$6.7^{+1.3}_{-1.1}$
N (Total)		1.19–2.24	1584	1366	1207	1486	1783	843	798	610
N (FeLoBAL)			1	2	8	9	15	19	22	19
f (FeLoBAL)			$0.06^{+0.02}_{-0.01}$	$0.2^{+0.2}_{-0.1}$	$0.7^{+0.3}_{-0.2}$	$0.6^{+0.3}_{-0.2}$	$0.8^{+0.3}_{-0.2}$	$2.3^{+0.7}_{-0.5}$	$2.8^{+0.7}_{-0.6}$	$3.1^{+0.9}_{-0.7}$
N (Total)	G09	0.55–2.15	2225	1817	1621	2030	2337	1252	1313	991
N (BI-LoBAL)			2	5	15	19	27	37	43	32
f (BI-LoBAL)			$0.09^{+0.12}_{-0.06}$	$0.3^{+0.2}_{-0.1}$	$0.9^{+0.3}_{-0.2}$	$0.9^{+0.3}_{-0.2}$	$1.2^{+0.3}_{-0.2}$	$3.0^{+0.6}_{-0.5}$	$3.3^{+0.6}_{-0.5}$	$3.2^{+0.7}_{-0.6}$

Note. The fractions are in percents.

to Dai et al. (2008b) for the detailed model. This assumes that the differential selection function for LoBALs and non-LoBALs in SDSS only depends on the different colors due to extinction and absorption troughs, which we believe is reasonable given our selected redshift range and the results of Allen et al. (2011). The model results are presented in Figure 4 (left), where the dashed lines are the intrinsic fractions of LoBALs and the solid lines connect the model results for the observed fraction of

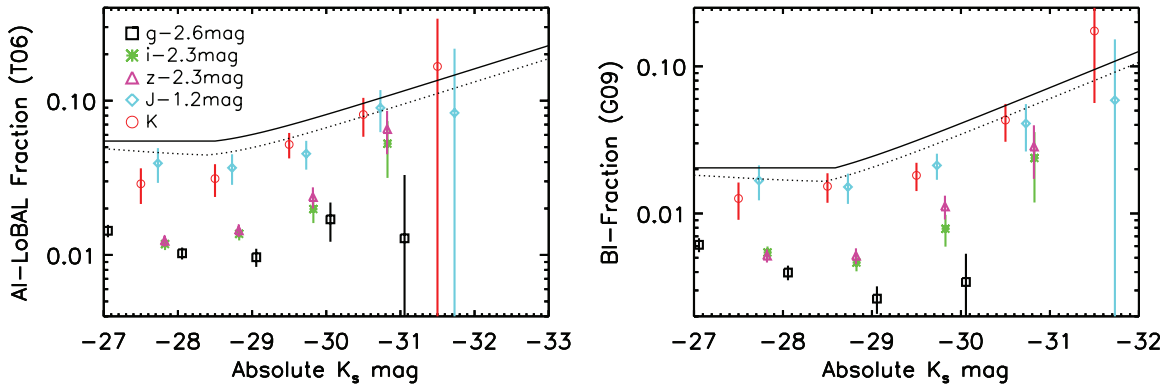

Figure 5. Left: the observed AI-LoBAL fractions as a function of optical and infrared luminosities. The g-, i-, z-, and J-band data are shifted right horizontally according to the mean color differences with respect to the K_s band. The fractions increase from the blue to red bands because of the selection biases, especially in shorter wavelength bands. We also find that the AI-LoBAL fractions increase from low to high luminosities, especially in the redder bands. The solid line shows the model intrinsic fractions from Model II, and the dotted line shows the model fractions in the K_s band from Model II that match well the observed K_s-band fractions at $K_s < -29.5$ mag. Right: same plot but for BI-LoBAL fractions from the G09 sample.

(A color version of this figure is available in the online journal.)

Table 2
Modeling Results for the Intrinsic Fractions of LoBALs Using the 2MASS and SDSS Data

	Model	AI T06	BI T06	BI G09	Fe T06
Intrinsic fraction (%)	I	6.4 ± 0.8	4.0 ± 0.6	2.8 ± 0.4	1.9 ± 0.4
χ^2/dof	I	13.4/6	9.0/6	21.6/6	16.9/6
δ	II	$0.41^{+0.06}_{-0.06}$	$0.43^{+0.07}_{-0.08}$	$0.65^{+0.07}_{-0.05}$	$0.81^{+0.07}_{-0.15}$
L_b in g mag	II	$-26.0^{+0.8}_{-0.5}$	$-26.0^{+0.9}_{-0.6}$	$-26.1^{+0.3}_{-0.2}$	$-26.1^{+0.2}_{-0.4}$
$\Phi_{0,\mathrm{LoBAL}}/\Phi_{0,\mathrm{Total}}$ (%)	II	$5.4^{+0.4}_{-0.3}$	$3.4^{+0.3}_{-0.3}$	$2.0^{+0.1}_{-0.1}$	$1.4^{+0.1}_{-0.2}$
χ^2/dof	II	2.67/4	1.58/4	2.88/4	2.41/4

Notes. Model I is a pure geometric model, where the only free parameter is the intrinsic fractions of LoBALs. Model II is a model with an additional power law at bright luminosities with respect to Model I as given in Equation (1). The parameter δ quantifies the difference in power-law slope of the additional component in the LoBAL luminosity function. The parameter L_b, expressed in intrinsic g-band magnitudes (not corrected for intrinsic obscuration), is the luminosity above which the additional power law kicks in. As a proxy for the overall LoBAL intrinsic fractions in Model II, we list the parameter $\Phi_{0,\mathrm{LoBAL}}/\Phi_{0,\mathrm{Total}}$, the ratio between the luminosity function normalizations of, respectively, LoBALs and the total quasar population.

Table 3
Modeling Results for the Intrinsic Fractions of LoBALs Using the FIRST Data

	Model	AI-LoBAL	BI-LoBAL	FeLoBAL
Intrinsic fraction (%)	Model I	8.4 ± 1.0	4.0 ± 0.7	3.6 ± 1.0
χ^2/dof		0.9/7	9.9/7	6.3/6

LoBALs. The square and filled circle symbols are the observed AI-LoBAL and BI-LoBAL fractions from T06. We also show the observed BI-LoBAL fractions from G09 as a comparison. The model produces acceptable fits to the data with $\chi^2/\mathrm{dof} = 1.5$ and 2.2 for BI-LoBALs and AI-LoBALs and measures intrinsic fractions of LoBALs of $4.0\% \pm 0.6\%$ for BI-LoBALs and $6.4\% \pm 0.8\%$ for AI-LoBALs. We note that the model fits the data from the bluer bands better than the redder bands, which is possible if there is a separate IR-luminous LoBAL population contributing to the LoBAL fractions, which we will discuss in detail later. The FeLoBAL fractions also show an increasing trend from the bluer g band to the redder K_s band (Figure 6, left). We list the model results for using a pure geometric model in Table 2.

We plot the AI-LoBAL, BI-LoBAL (G09), and FeLoBAL fractions as a function of NIR and optical luminosities in Figures 5 and 6 (right). In general, we find that the fractions are larger in the redder bands than bluer bands, consistent with the results found above. We also find that there is an increasing trend in LoBAL fractions as a function of luminosity, especially in the redder 2MASS bands. The bluer g band does not show such a trend. This trend, especially in the redder bands, is not observed in BALQSOs in general (Dai et al. 2008b). Besides the bluer bands, which are more affected by the obscuration, the other bands have similar slopes for the increase of LoBAL fractions as a function of luminosity. However, the data at the luminous end have large uncertainties. Early IR surveys of LoBALs (with sample sizes $\sim$10) typically found LoBAL fractions of $\gtrsim$10% (e.g., Boroson & Meyers 1992), higher than our intrinsic fraction. It is possible that these early IR surveys have higher flux limits that can only probe the most IR-luminous population, where we also find a large LoBAL fraction of $\gtrsim$10%.

It is possible that the increasing fraction with luminosity is a result of increasing signal-to-noise ratio (S/N) spectra for quasars, such that it is more likely to identify sources as BALQSOs. This effect has been discussed previously (Knigge et al. 2008; G09; Allen et al. 2011). However, our sample only probes the most luminous quasars after applying the 2MASS flux limits, and in this regime, the effect due to S/N is small. For example, in Figure 11 of Allen et al. (2011), the C IV BAL fraction is a constant for the most luminous quasars. If the trend of increasing fraction with luminosity is really due to the S/N of quasar spectra, it indicates that the intrinsic LoBAL fractions are close to $\sim$18%, however with large uncertainties. In the rest of the paper, we assume that the S/N has a small effect on the observed fractions in the luminosity range of our sample.

If the non-constant behavior shown by LoBAL fractions as a function of luminosity is actually induced by a true underlying physical effect, we then need to look for models beyond the standard, basic geometric model. In the following, we thus present a luminosity-dependent LoBAL model (Model II) that assumes that the intrinsic probability of catching a LoBAL in a luminous bin is higher than in fainter regimes. In other words, the duty cycle of a LoBAL phase with respect to a non-LoBAL phase is assumed to increase with increasing luminosity. Mathematically, this is achieved by assuming that

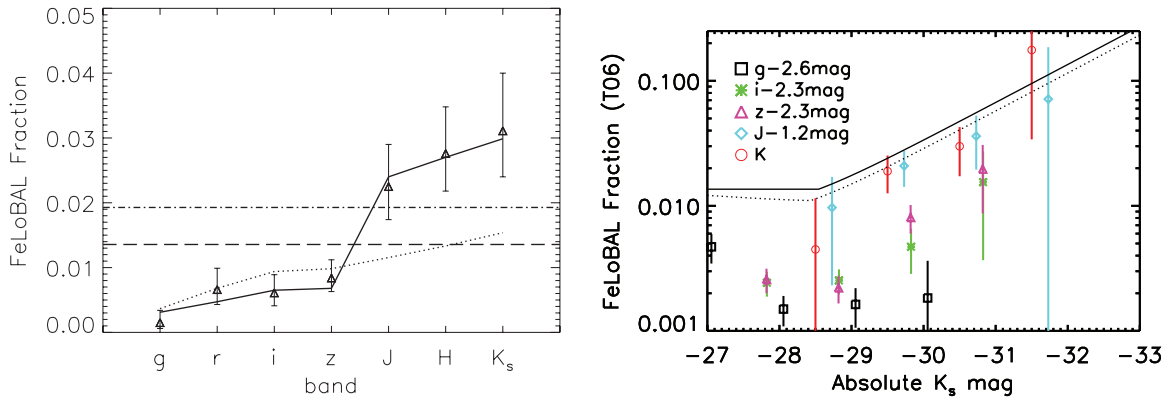

Figure 6. Left: observed FeLoBAL fractions from the g to K_s bands. The triangles are the data. The dotted line is the best-fit observed fractions from a pure geometric model, Model I, and the dot-dashed line shows the intrinsic fraction from this model. The solid line is the best-fit observed fractions from Model II, and the dashed line shows the ratio of luminosity functions' normalizations as a proxy for intrinsic fractions. Right: observed FeLoBAL fractions as a function of optical and infrared luminosities. The solid line is the model intrinsic FeLoBAL fraction from Model II, and the dotted line shows the model fraction in the K_s band from Model II.
(A color version of this figure is available in the online journal.)

the intrinsic luminosity function of LoBALs, besides the lower normalization, has a somewhat different shape at the brightest luminosities. We also assume that the differences only apply in the 2MASS bands. In the specifics, we assume that the bright end of the LoBAL luminosity function is described by a two-power-law function

$$\Phi(L) \propto \begin{cases} L^{-\alpha} & \text{if } L < L_b \text{ (in } g \text{ mag)} \\ L^{-(\alpha+\delta)} & \text{if } L \geqslant L_b \text{ (in } g \text{ mag)} \end{cases} \quad (1)$$

with a break at $L = L_b$ above which the luminosity function gets *less* steep by an amount $\delta > 0$ with respect to the luminosity function characterizing all quasars in the 2MASS bands. Compared with Model I, Model II has two additional free parameters, L_b and δ. We express this additional break L_b in g magnitudes to easily compare with the original break in the quasar luminosity function ($L_* \sim -25$ mag at $z = 1.5$), which is also expressed in the g band in Richards et al. (2005). Thus, the LoBAL luminosity function can be considered as adding a luminosity-dependent component on top of a fraction of the non-BAL luminosity function. Since we construct luminosity functions in other bands using the mean color differences of these bands from the g band, we introduce only two additional parameters in this model. Model II implies that the ratio of LoBAL/total will not be a constant but depends on luminosities and wavelengths. Physically, Model II can be thought of as a combination of a geometric model, given by the cumulative and/or median fraction of LoBALs within an AGN sample below a certain luminosity, with an "evolutionary" component, correlated with luminosity. The increasing probability of finding LoBALs at higher luminosities could in fact be linked, for example, to the idea of LoBALs being young luminous quasars at the stage of becoming powerful enough to blow out the obscuring material or to simply generate large-scale winds (see Section 1).

We present the best fit of Model II in Figures 4 (right) and 6 (left) and list the fitting results in Table 2. In all three cases, we find that the models fit the observed fractions well and better than Model I. We find that for Model II all the resulting χ^2/dof < 1, and thus fully acceptable, at variance with what was obtained with Model I. We find that, despite its simplicity, Model II provides in fact an impressively good fit to the data. We have also experimented with other models but never found the same level of success. For example, we do not find a better fit than Model I by forcing the brightening of the LoBAL luminosity functions to apply in all bands, which suggests that the luminosity-dependent component of LoBALs has a different spectral energy distribution (SED) than the rest of LoBALs. In the case of Model II, one cannot appropriately deal with absolute intrinsic fractions as the duty cycle of LoBALs, by construction, is luminosity dependent. As a proxy for overall LoBAL fractions (integrating by luminosity), we list in Table 2 the ratios of the normalizations between the LoBAL and total luminosity functions for all quasars. These ratios, from around 5% for the AI classification down to 1% for FeLoBALs, are comparable to but lower than the global geometric fractions constrained in Model I. We find that all data sets force the models to flatten the intrinsic LoBAL luminosity function around $L_b \sim -26$ mag. Moreover, the degree of flattening is significant for all models, constrained to be around $\delta \sim 0.4$–0.8. Although we find a larger δ value for FeLoBALs, the associated uncertainty is also larger. Thus, we find both L_b and δ in Model II to be roughly consistent among them for the different LoBAL cases within the uncertainties.

After obtaining the best-fit models, we plot the model intrinsic fractions (solid lines) of LoBALs as a function of K_s-band luminosity in Figures 5 and 6 (right), for AI-LoBALs, BI-LoBALs (G09), and FeLoBALs, respectively. The intrinsic fractions at different luminosities represent an envelope for observed fractions. The observed fractions are below the models since they are biased with different degrees. The K_s-band fractions are closest to the model, since there is less obscuration in the K_s band, and they match well to the model K_s-band fractions shown in dotted lines in $M_{K_s} < -29.5$ mag.

3.3. Radio Properties of LoBALs

We show the fraction of LoBALs as a function of the 1.4 GHz radio luminosity in Figure 7 (left). In the $0.5 \leqslant z \leqslant 2.15$ redshift range, we find 2650, 95, and 49 matches in FIRST for the SDSS quasars, AI-LoBALs, and BI-LoBALs, respectively. In the $1.19 \leqslant z \leqslant 2.24$ redshift range, we find 1621 and 19 matches in FIRST for the SDSS quasars and FeLoBALs, respectively. We find that the fraction of LoBALs decreases with increasing radio luminosities. This is true in all of the sub-samples of LoBALs (BI-LoBALs, AI-LoBALs, AINB-LoBALs, and FeLoBALs). We do not show the AINB-LoBAL fractions in Figure 5 for clarity, but the numbers can be obtained by subtracting the

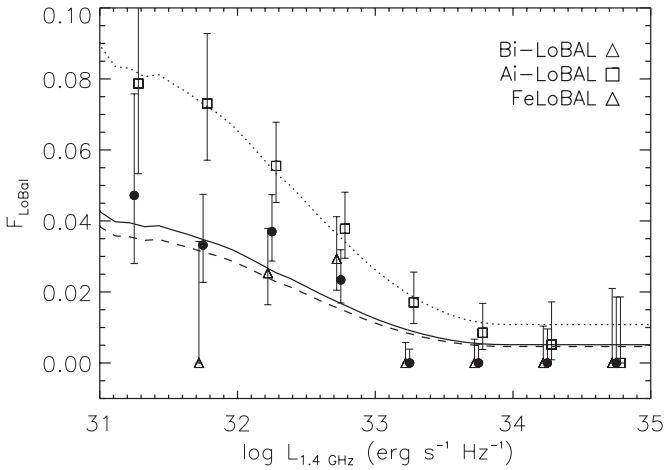

Figure 7. Fractions of LoBALs and FeLoBALs as a function of the 1.4 GHz radio luminosity. The data are slightly shifted horizontally for clarity. At the low-luminosity end, the fractions are consistent with or even higher than the intrinsic fractions modeled through the NIR and optical bands. The fractions are significantly smaller at high radio luminosities. Using a geometric model for LoBALs (solid, dotted, and dashed lines for BI-LoBALs, AI-LoBALs, and FeLoBALs, respectively), we are able to fit the trend and obtain intrinsic fractions of 4.0% ± 0.7%, 8.4% ± 1.0%, and 3.6% ± 1.0% for BI-LoBALs, AI-LoBALs, and FeLoBALs, respectively.

BI-LoBAL fractions from the AI-LoBAL fractions. In addition, the LoBAL fraction at the low radio luminosity end is consistent with the intrinsic fraction obtained in Section 3.2. This is not unexpected since there is also little obscuration in the radio band. These two features are similar to BALQSOs (Shankar et al. 2008b).

The decrease in the LoBAL fractions as a function of radio luminosity can be easily explained under a fully geometric model for LoBALs, if we assume that LoBALs are viewed in the lines of sight close to the accretion disk, while the boosted radio emission is viewed close to the polar direction. We test this model following Shankar et al. (2008b). We assume that the radio emission is composed of one weaker uniform component and another beamed component in the polar direction. LoBALs are modeled to be within a solid angle close to the equatorial plane, where the open angle is a free parameter. The rest of the parameters, such as the slope of the luminosity function, Lorentz factor, and maximum beaming angle, are all fixed according to the literature (Urry & Padovani 1991, 1995; De Zotti et al. 2005; Richards et al. 2006; Jiang et al. 2007; Padovani et al. 2007). Please refer to Shankar et al. (2008b) for the detailed model.

Using this model, we find good fits to the data with χ^2/dof = 1.4, 0.12, and 1.0 for BI-LoBALs, AI-LoBALs, and FeLoBALs, respectively, and the corresponding intrinsic fractions of these objects are 4.0% ± 0.7%, 8.4% ± 1.0%, and 3.6% ± 1.0% in quasars (Table 3). These fractions are consistent with and even higher than the LoBAL fractions obtained using a pure geometric model (Model I). The measured fractions at low radio luminosities are similar to the intrinsic fractions measured in the IR, a reassuring result that further supports the idea that little absorption occurs in the radio band, and thus the cumulative fractions in the radio bands should be larger than those inferred in the optical.

The data in the radio band are accurately described enough by a basic geometric model with no need for any additional component. Physically this implies that irrespective of evolutionary transitions that may boost the appearance of LoBALs in some phase, there is a preferential orientation for radio LoBALs to be viewed in a region close to the equatorial plane. Moreover, from the radio flux versus K_s-magnitude plots in Figures 1 and 2, it is evident that, despite the large scatter, the K_s-bright LoBALs usually have relatively faint radio fluxes. Therefore, any modest additional luminosity/evolutionary component for LoBALs that acts in boosting the observed fraction of LoBALs in the reddest bands should mainly show up at faint radio fluxes, where the fraction of radio LoBALs is anyway already high. Overall, it is not unexpected that a pure geometric model, which already represents a good physical approximation for the bulk of the LoBAL luminosity distribution in the optical/NIR bands, is also sufficient to reproduce the radio data.

Table 4
Final Intrinsic Fractions of LoBALs by Combining the Two Methods

	Model	AI-LoBAL	BI-LoBAL	FeLoBAL
Intrinsic fraction (%)	Model I	7.1 ± 0.6	4.0 ± 0.5	2.1 ± 0.3

4. SUMMARY AND DISCUSSION

We find significantly high fractions of LoBALs in the quasar population compared to the values obtained using optical data only. For example, the BI-LoBAL and AI-LoBAL fractions in the optical data were measured as 0.55% and 1.31% (T06), while our results are 5–7 times larger. Although the final intrinsic fractions depend on the choice of catalogs, the overall trend is found to be the same. For example, we perform a similar analysis to the BI-LoBALs from the G09 sample and also find large intrinsic LoBAL fractions. Although there is a systematic offset between the BI-LoBAL fractions from the T06 and G09 samples, the overall trend for the observed fractions is the same. Our intrinsic fractions are obtained using two independent methods, one from the NIR and optical data and the other from the radio data, and the results are mutually consistent between the two methods. Combining the estimates from the two methods using the least-squares (minimum variance) method, we find that the intrinsic fractions for BI-LoBALs, AI-LoBALs, and FeLoBALs are 4.0% ± 0.5%, 7.1% ± 0.6%, and 2.1% ± 0.3%, respectively, using a pure geometric model. We also find evidence that the intrinsic fractions in the NIR bands increase even further, possibly suggesting an additional evolutionary/luminosity-dependent component characterizing the LoBAL population. A model in which the intrinsic LoBAL luminosity function flattens above $L_b \leqslant -26$ mag provides an excellent fit to all data sets (see Table 4 for all the results of the χ^2 fitting). This additional break for LoBALs is at a slightly higher luminosity than the original break $L_* \sim -25$ at $z = 1.5$ of the quasar luminosity function (Richards et al. 2005). Thus, if one of the breaks is smooth enough, they can be merged into one break, and the LoBAL luminosity function will just have a flatter slope at the high-luminosity end. A luminosity-dependent component does not necessarily require a different SED, since this component can be from pure number differences at different luminosities. However, our fitting results in Model II prefer different SEDs for LoBALs because the fits require that the luminosity-dependent component be only in the 2MASS bands. Recently, Lazarova et al. (2012) compared the mid-IR properties of a sample of LoBALs and non-BALs and found no significant difference in their SEDs, which may contradict our findings. We note that the sample size of Lazarova et al. (2012) is much smaller than the ones used in this paper. Combined with all results, it is possible that the luminosity-dependent component

of LoBALs can be physically related to a model with larger LoBAL opening angles for higher luminosity quasars, which has been suggested in simulations (e.g., Proga et al. 2008).

Although we find significantly larger intrinsic fractions of LoBALs, not unexpected considering the large obscuration observed in LoBALs (e.g., Sprayberry & Foltz 1992), they still represent a small portion of the total population. For comparison, we find that the intrinsic fractions BI-BALQSOs and AI-BALQSOs are, respectively, $20\% \pm 2\%$ and $43\% \pm 2\%$ (Dai et al. 2008b), i.e., the LoBALs are about 20% of BALQSOs.

Our method of calculating the intrinsic fractions of BALQSOs still depends on the completeness of optical quasar surveys. The fraction of quasars that do not enter the optical surveys was not accounted for in this or our previous results. It was estimated that SDSS has a very high degree of completeness at $z < 2.2$ and $i < 19.1$ mag (Richards et al. 2002). However, the latter estimate was based on simulations performed using "normal" quasars, so it cannot be directly applied to heavily obscured LoBALs. We thus expect the fraction of LoBALs missing to still be significant and further raise the estimates provided here. For example, Meusinger et al. (2012) used self-organizing Kohonen maps to find unusual quasars with a 41% fraction of BALs and large LoBAL fractions. We also caution, though, that the nature of the obscured quasars is still uncertain, and it is not clear whether the ultraviolet spectra of these quasars would still show BALQSOs even in the case of heavy obscuration. Therefore, the fractions quoted in our paper represent conservative estimates based on observations. There are also other uncertainties such as the redshift dependence of our modeling results and the dispersion in LoBAL obscuration, where we use simplified averages in our simulations while the real data have distributions. These issues still need to be addressed in future analyses.

The LoBAL fractions in the radio band are particularly interesting, since we find that the LoBAL fractions decrease with increasing radio luminosities. This confirms the early result of Becker et al. (2000) with about a dozen LoBALs. The trend is similar to that found in the total BALQSO population (Shankar et al. 2008b). This trend found in both the total BALQSO population and LoBALs suggests that the majority of LoBALs and BALQSOs can be united under a similar physical scheme. In Shankar et al. (2008b), we favored a geometric model to interpret the trend. Applying the geometric model of Shankar et al. (2008b) to LoBALs, we can successfully reproduce the luminosity-dependent fractions for BI-LoBALs, AI-LoBALs, and FeLoBALs in the radio band. Polar BALQSOs/outflows (Zhou et al. 2006; Ghosh & Punsly 2007; Dai et al. 2008a) present a challenge to our results; however, these objects are rare and we are uncertain about their implications to the total quasar population. A modification of the geometric model to have both disk and polar outflows (e.g., Borguet & Hutsemékers 2010) may be needed to incorporate these objects. We also note that LoBALs dominate this population of polar BALQSO candidates (Ghosh & Punsly 2007).

There are other indications, such as the association with ULIRGs, radio spectra, and large covering fractions from spectral modeling, arguing that LoBALs belong to an earlier evolutionary stage of quasar population (Montenegro-Montes et al. 2008; Lipari et al. 2009; Farrah et al. 2012; Westmoquette et al. 2012). Urrutia et al. (2009) studied the fraction of LoBALs in the dust-reddened quasars at high redshift, finding that all except one are LoBALs, supporting the young nature of LoBALs. However, the authors also noted that their selection method may be biased favoring LoBALs since they are associated with large dust reddening. In our study, we find that LoBALs and BALQSOs are similar in most aspects, except that the fraction of LoBALs increases with increasing NIR luminosities. This is not consistent with BALQSOs in general, because the BALQSO fractions are mostly constant with increasing NIR luminosities for AI-BALQSOs (Dai et al. 2008b). At the NIR-luminous end, the observed LoBAL fraction is higher, although with large uncertainties, than the intrinsic fraction that we obtain for a pure geometric model.

It is possible that a portion of NIR-luminous LoBALs are special compared to the rest of the population, and at an early evolutionary stage of the quasar cycle, corresponding to the targets studied in Farrah et al. (2012) and Urrutia et al. (2009) correcting for absorption. This will reconcile some observations supporting the young quasar interpretation for LoBALs. In fact, the combination of a short early evolution model and a longer stationary phase with large covering factor (the "geometric" phase) could simultaneously account for many of the differences and similarities between LoBALs and HiBALs. The longer-lived geometric phase mainly sets the intrinsic fractions of BALQSOs of various species and the measured fraction as a function of their radio luminosities. If there is some small spherical outflow component at early times, this might also explain the predominance of LoBALs among the rare polar BALQSOs.

We acknowledge the anonymous referee for helpful comments. X.D. acknowledges financial support by the NASA Grant NNX11AD09G. F.S. acknowledges partial support from the Alexander von Humboldt Foundation and a Marie Curie Fellowship.

REFERENCES

Allen, J. T., Hewett, P. C., Maddox, N., Richards, G. T., & Belokurov, V. 2011, MNRAS, 410, 860
Becker, R. H., Fan, X., White, R. L., et al. 2001, AJ, 122, 2850
Becker, R. H., White, R. L., Gregg, M. D., et al. 2000, ApJ, 538, 72
Becker, R. H., White, R. L., & Helfand, D. J. 1995, ApJ, 450, 559
Borguet, B., & Hutsemékers, D. 2010, A&A, 515, A22
Boroson, T. A., & Meyers, K. A. 1992, ApJ, 397, 442
Brotherton, M. S., van Breugel, W., Smith, R. J., et al. 1998, ApJ, 505, 7
Canalizo, G., & Stockton, A. 2000, AJ, 120, 1750
Casebeer, D., Baron, E., Leighly, K., Jevremovic, D., & Branch, D. 2008, ApJ, 676, 857
Dai, X., Mathur, S., Chartas, G., Nair, S., & Garmire, G. P. 2008a, AJ, 135, 333
Dai, X., Shankar, F., & Sivakoff, G. R. 2008b, ApJ, 672, 108
De Zotti, G., Ricci, R., Mesa, D., et al. 2005, A&A, 431, 893
Di Matteo, T., Springel, V., & Hernquist, L. 2005, Nature, 433, 604
Elvis, M. 2000, ApJ, 545, 63
Farrah, D., Urrutia, T., Lacy, M., et al. 2012, ApJ, 745, 178
Francis, P. J., Hooper, E. J., & Impey, C. D. 1993, AJ, 106, 417
Gallagher, S. C., Brandt, W. N., Chartas, G., & Garmire, G. P. 2002, ApJ, 567, 37
Ganguly, R., & Brotherton, M. S. 2008, ApJ, 672, 102
Gehrels, N. 1986, ApJ, 303, 336
Ghosh, K. K., & Punsly, B. 2007, ApJ, 661, L139
Gibson, R. R., Jiang, L., Brandt, W. N., et al. 2009, ApJ, 692, 758
Granato, G. L., De Zotti, G., Silva, L., Bressan, A., & Danese, L. 2004, ApJ, 600, 580
Green, P. J., Aldcroft, T. L., Mathur, S., Wilkes, B. J., & Elvis, M. 2001, ApJ, 558, 109
Hewett, P. C., & Foltz, C. B. 2003, AJ, 125, 1784
Hopkins, P. F., Hernquist, L., Cox, T. J., et al. 2006, ApJS, 163, 1
Jiang, L., Fan, X., Ivezić, Ž., et al. 2007, ApJ, 656, 680
Knigge, C., Scaringi, S., Goad, M. R., & Cottis, C. E. 2008, MNRAS, 386, 1426
Lazarova, M. S., Canalizo, G., Lacy, M., & Sajina, A. 2012, ApJ, 755, 29
Lipari, S. 1994, ApJ, 436, 102
Lipari, S., Sanchez, S. F., Bergmann, M., et al. 2009, MNRAS, 392, 1295

Liu, Y., Jiang, D. R., Wang, T. G., & Xie, F. G. 2008, MNRAS, 391, 246
Maddox, N., Hewett, P. C., Warren, S. J., & Croom, S. M. 2008, MNRAS, 386, 1605
Meusinger, H., Schalldach, P., Scholz, R.-D., et al. 2012, A&A, 541, A77
Montenegro-Montes, F. M., Mack, K.-H., Vigotti, M., et al. 2008, MNRAS, 388, 1853
Padovani, P., Giommi, P., Landt, H., & Perlman, E. S. 2007, ApJ, 662, 182
Proga, D., Ostriker, J. P., & Kurosawa, R. 2008, ApJ, 676, 101
Reichard, T. A., Richards, G. T., Hall, P. B., et al. 2003, AJ, 126, 2594 (R03)
Richards, G. T., Croom, S. M., Anderson, S. F., et al. 2005, MNRAS, 360, 839
Richards, G. T., Fan, X., Newberg, H. J., et al. 2002, AJ, 123, 2945
Richards, G. T., Strauss, M. A., Fan, X., et al. 2006, AJ, 131, 2766
Scaringi, S., Cottis, C. E., Knigge, C., & Goad, M. R. 2009, MNRAS, 399, 2231
Schneider, D. P., Hall, P. B., Richards, G. T., et al. 2005, AJ, 130, 367
Shankar, F., Cavaliere, A., Cirasuolo, M., & Maraschi, L. 2008a, ApJ, 676, 131
Shankar, F., Dai, X., & Sivakoff, G. R. 2008b, ApJ, 687, 859
Shankar, F., Lapi, A., Salucci, P., De Zotti, G., & Danese, L. 2006, ApJ, 643, 14
Shankar, F., Sivakoff, G. R., Vestergaard, M., & Dai, X. 2010, MNRAS, 401, 1869
Skrutskie, M. F., Cutri, R. M., Stiening, R., et al. 2006, AJ, 131, 1163
Sprayberry, D., & Foltz, C. B. 1992, ApJ, 390, 39
Stocke, J. T., Morris, S. L., Weymann, R. J., & Foltz, C. B. 1992, ApJ, 396, 487
Trump, J. R., Hall, P. B., Reichard, T. A., et al. 2006, ApJS, 165, 1
Urrutia, T., Becker, R. H., White, R. L., et al. 2009, ApJ, 698, 1095
Urry, M., & Padovani, P. 1991, ApJ, 371, 60
Urry, M., & Padovani, P. 1995, PASP, 107, 803
Voit, G. M., Weymann, R. J., & Korista, K. T. 1993, ApJ, 413, 95
Westmoquette, M. S., Clements, D. L., Bendo, G. J., & Khan, S. A. 2012, MNRAS, 424, 416
Weymann, R. J., Morris, S. L., Foltz, C. B., & Hewett, P. C. 1991, ApJ, 373, 23
Zhou, H., Wang, T., Wang, H., et al. 2006, ApJ, 639, 716